

# Experimental Observation of Quantum Chaos in a Beam of Light

G. B. Lemos,\* R. M. Gomes, S. P. Walborn, P. H. Souto Ribeiro, and F. Toscano  
*Instituto de Física, Universidade Federal do Rio de Janeiro,  
Caixa Postal 68528, Rio de Janeiro, RJ 21941-972, Brazil*

**In classical physics, chaotic behavior constitutes the majority of all possible dynamics of isolated conservative systems. Because every physical process ultimately follows the rules of quantum mechanics, in principle one should frequently observe a corresponding quantum chaotic evolution, with all the signatures of classical chaos [1]. However, the fragile quantum coherence effects quickly vanish even under weak interactions of the system with its surroundings, restoring classical behavior. The loss of coherence occurs even faster for chaotic systems [2], and is hard to avoid, even in well-controlled laboratory conditions. As a consequence, few experiments have been performed with quantum systems that have a classical chaotic counterpart [3–12]. Here we report the implementation of the quantum Kicked Harmonic Oscillator, a paradigmatic system for the study of quantum chaos. Using an all optical setup that is essentially decoherence-free, we are able to observe the non-linear dynamics through the direct measurement of the time-evolved Wigner function. Completely controllable experimental parameters allow us to adjust the system continuously from regular to completely chaotic dynamics, as well as the effective Planck constant, the key parameter associated to the quantum-classical transition. We show the utility of our approach by experimentally investigating the decoherence induced by our chaotic system on a quantum bit. Our scheme can be employed in a rich variety of experimental investigations of non-linear quantum systems.**

Chaotic classical systems have the characteristic trait of being extremely sensitive to initial conditions. This behavior, together with the experimental imprecision of the initial conditions, cause these deterministic systems to be inherently unpredictable. The question as to how classical chaotic dynamics manifests itself in quantum mechanics is an important branch in the field of quantum chaos. In addition to fundamental questions concerning the correspondence principle and the semi-classical limit of quantum mechanics, a number of intriguing quantum-dynamical features have been uncovered. Prominent examples are dynamical localization [13], the quantum suppression of classical diffusion, and the enhancement of the tunneling rate in the presence of chaos in the corresponding classical dynamics [4].

The simplest systems that exhibit all the intriguing manifestations of classical chaos in their quantum dynamics are periodic time-dependent Hamiltonian (Floquet) systems, and are thus the most vastly studied systems in the discipline of quantum chaos [14]. The quantum evolution up to discrete

time  $t = nT$  is described by the quantum map

$$|\psi(n)\rangle = U^n |\psi(0)\rangle, \quad (1)$$

where  $n$  is an integer and the Floquet operator  $U$  describes the unitary quantum evolution in the time period  $T$ . They have been extensively investigated from a theoretical viewpoint, quantum maps corresponding to classical chaotic behavior have been studied experimentally in different systems [3–11]. This is due primarily to the difficulty in manipulating quantum systems and preserving them from decoherence, the interaction between a quantum system and the environment [2].

There have been a few theoretical proposals to realize quantum chaotic maps using optics [15–17]. To our knowledge, these experiments have never been carried out, and more elaborate evolutions may not be possible or require difficult or complex optical devices. Here we present an optical implementation of the quantum kicked harmonic oscillator (KHO), an archetype in the study of quantum chaos. The dynamics are observed by direct measurement of the Wigner function, and all relevant parameters are easily controlled. We then illustrate the utility of this experimental system studying the loss of coherence in different chaotic regimes.

The quantum KHO serves as a model for charges moving in orthogonal magnetic and time-dependent electric fields [18], for the electronic transport in semiconductor lattices [19, 20], and for trapped ions addressed by a periodic standing laser field [21]. Its evolution is described by the map (1), where the iteration operator is

$$U_{\text{KHO}} = R_\alpha V_K. \quad (2)$$

The operator  $R_\alpha$  describes the usual evolution of a quantum harmonic oscillator parameterized by  $\alpha = \omega T$ , where  $\omega$  is the oscillator frequency, and  $T$  the interval between the periodic perturbations.  $V_K$  describes a periodic perturbation that corresponds to a potential  $K \cos(Q + \phi)$ . The quantum KHO presents a rich variety of dynamical regimes [22, 23], depending on the perturbation amplitude,  $K$ . For  $\alpha = 2\pi/m$ , with  $m \in \{1, 2, 3, 4, 6\}$ , the quantum system can present diffusion in energy; while for other values of  $\alpha$ , an interesting transition from dynamical localization to delocalization is observed in numerical simulations [24, 25].

The Poincaré section of the classical KHO for  $\alpha = 2\pi/m$  is characterized by the appearance of a “stochastic web” associated to the chaotic behavior, with periodic regions corresponding to essentially regular dynamics in between [18], as illustrated in Fig. 2. The size of the web and the perturbation of the regular dynamics inside the periodic regions is governed



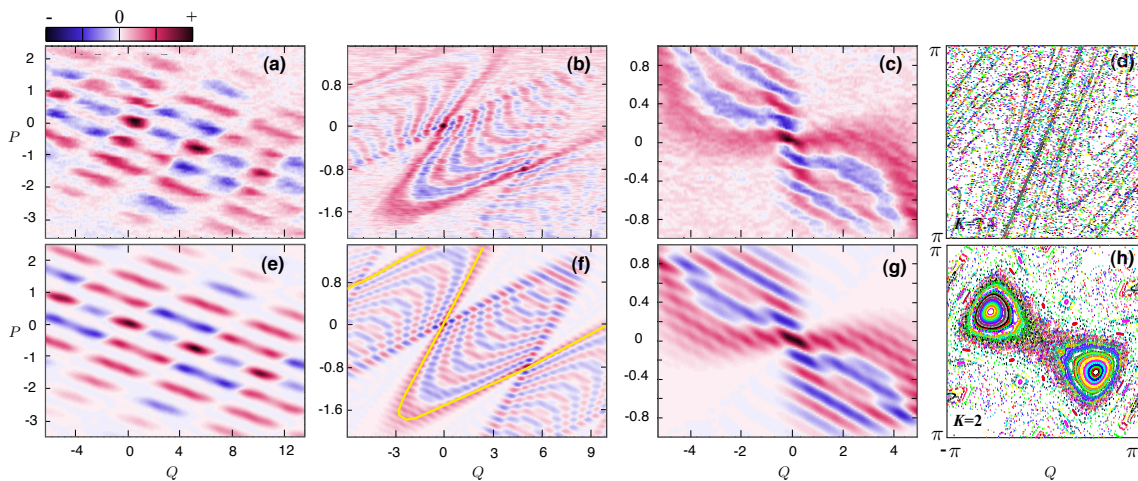


FIG. 2: **Experimental and theoretical Wigner distributions for a single iteration of the KHO map and associated classical Poincaré sections.** **a-c**, directly measured optical Wigner distributions, **e-g**, corresponding numerical predictions. For (a) and (e), the relevant parameters are  $K = 7.4$  and  $\hbar_{\text{eff}} = 4.72$ . For (b) and (f),  $K = 7.4$  and  $\hbar_{\text{eff}} = 0.9$ . The yellow line outlines the phase space manifold that is the skeleton of both the quantum and the classical distributions corresponding to the KHO Hamiltonian, **c, g**, For  $K = 2$  and  $\hbar_{\text{eff}} = 0.9$ , **d, h**, the associated classical phase space is illustrated by the Poincaré sections. In all cases the harmonic evolution parameter is  $\alpha = \pi/3$ .

where  $A$  is a normalization constant. We use an interferometric method [30] to measure the Wigner function, as described in the supplementary material.

Two spherical lenses ( $L1$  and  $L2$ ) of focal length  $f = 350$  mm are used to map the output state of the KHO system  $|\psi(n)\rangle$  from the transverse plane at position  $z_0$  to the input mirror of the Sagnac interferometer. A Dove prism (DP1) tilted at a  $45^\circ$  angle is used to swap the horizontal and vertical coordinates, because for convenience the quantum kicked Hamiltonian is implemented in the vertical axis, while the Wigner measurement is performed in the horizontal. The second PBS (PBS2) and the first half wave plate (HWP1) are used to keep the beam linearly polarized before entering the Sagnac interferometer.

Figs. 2(a-c) show three experimental Wigner distributions for a single iteration ( $n = 1$ ) of the quantum map (2) applied to an initial squeezed Gaussian state  $|\Psi(0)\rangle$  centered at the phase space origin, which is a fixed point of the classical KHO map. The theoretical Wigner distributions are shown for comparison in Figs. 2(e-g). All three cases correspond to the harmonic evolution  $\alpha = \pi/3$ . Figs. 2(a, e) and (b, f) show results for the kick amplitude  $K = 7.4$ . One can see that the smaller  $\hbar_{\text{eff}} = 0.9$  used in Fig. 2(b, f) enables finer interference patterns to appear, in comparison to Fig. 2(a, e) with  $\hbar_{\text{eff}} = 4.72$ . In the chaotic regime, stretching and folding of the Wigner distribution  $\mathcal{W}(Q, P)$  gives rise to fine oscillatory phase-space structure [31], known as sub-Planck structure, in a scale that is proportional to  $\hbar_{\text{eff}}^2$ . These in-

terference patterns are a quantum signature that can only be wiped out by decoherence [32, 33]. However, as the effective Planck constant approaches the semiclassical limit ( $\hbar_{\text{eff}} \rightarrow 0$ ), one identifies the concentration of the phase-space distribution over the evolved classical curve (yellow line), that is the skeleton of both the Wigner function and the corresponding classical probability distribution under KHO evolution of an initial Gaussian wave packet [34, 35].

The quantum sub-Planck and underlying classical structure associated to the evolution of Gaussian wave packets in chaotic systems can be observed for two final states corresponding to weak chaos  $K = 2$  in Figs. 2(c, g) and strong chaos  $K = 7.4$  in Figs. 2(b, f). We notice the typical stretching and folding of the classical manifold that supports the Wigner distribution in these chaotic regimes [34, 35]. Every two points on this classical manifold generate an interference fringe halfway between the chord that joins them with a frequency that is proportional to the length of this chord [34]. By comparing Fig.2(b, f) to Fig.2(c, g), one can observe that the skeleton of the Wigner function after one kick for  $K = 7.4$  folds in phase space in a more pronounced manner due to the more chaotic dynamics (see the corresponding Poincaré sections in Fig. 2(d) and 2(g)).

Fig. 3 displays experimental Wigner distributions for the first three iterations of the KHO map (2) for the same initial state  $|\Psi(0)\rangle$ . In this case we changed the harmonic evolution to  $\alpha = 2\pi/3$ . Figs. 3(a-c) show the evolution for essentially regular dynamics, with  $\hbar_{\text{eff}} = 0.42$  and  $K = 0.75$ . The

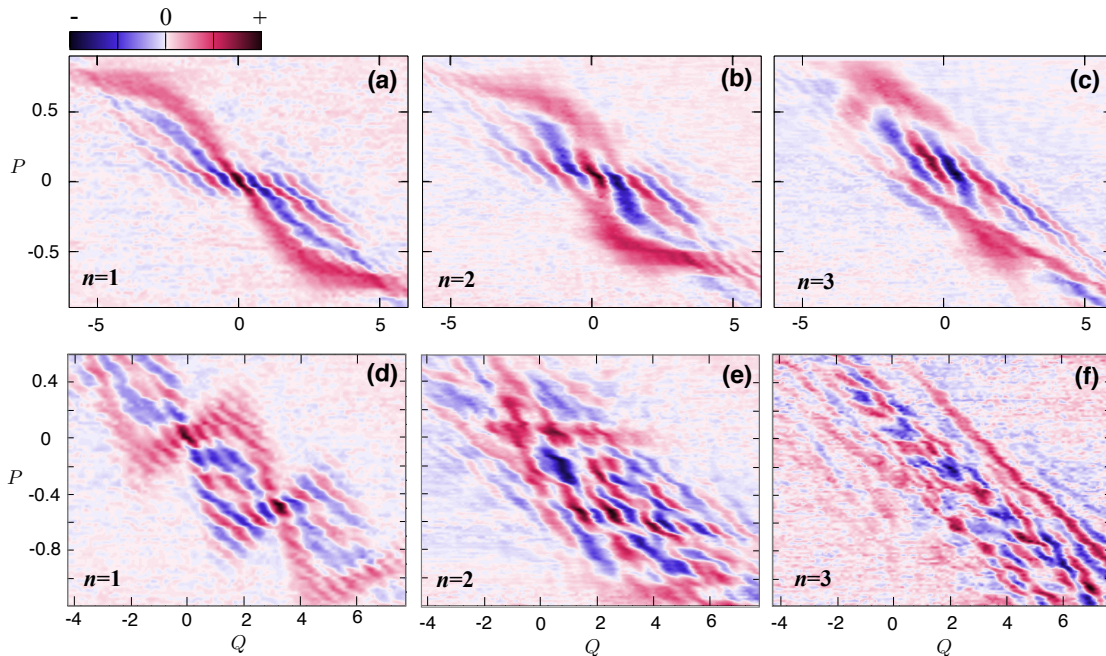


FIG. 3: **Experimentally obtained Wigner distributions corresponding to the first three iterations of the KHO map.** **a-c**, The case of regular dynamics, with  $K = 0.75$ , and  $\hbar_{\text{eff}} = 0.42$ . **d-f**, Weak chaos regime, with  $K = 2$ , and  $\hbar_{\text{eff}} = 0.9$ . In all cases  $\alpha = 2\pi/3$ .

Wigner function, initially centered at the origin, spreads over a limited area in phase space. Conversely, dynamical spreading of the Wigner distribution is observed for the weak chaotic regime in Figs. 3(d-f) with  $\hbar_{\text{eff}} = 0.9$  and  $K = 2$ .

As an example of the utility and versatility of our approach, we experimentally studied the loss of coherence by a polarization qubit interacting with a chaotic environment. The results are shown in Fig. 4 (see supplementary material for methods). Taking advantage of the fact that the SLM only imprints a phase on the horizontal polarization component, a dephasing-type coupling was implemented between the polarization and the transverse spatial degrees of freedom of the laser beam. Decoherence produced by the interaction with only a few environmental degrees of freedom is the main obstacle to quantum computing when the system of interest is well isolated [36–38]. In this case, entropy production and irreversible loss of coherence are directly related to chaotic dynamics of the environmental degrees of freedom [38–41].

In this case, the quantum KHO, implemented in the spatial degrees of freedom acts as an environment for the qubit encoded in the polarization state. By preparing the incoming beam in the linear diagonal polarization state, the polarization and the transverse spatial variables become entangled, leading to loss of purity of the polarization state. We studied this process as a function of  $K$  and  $\hbar_{\text{eff}}$ .

In Figs. 4(a) and (b), the purity of the polarization state is plotted as a function of the number of iterations of the KHO map. The different curves correspond to different values of  $\hbar_{\text{eff}}$ . Fig. 4(a) shows the case in which the KHO has regular dynamics ( $K = 0.5$ ), and Fig. 4 (b) is for essentially

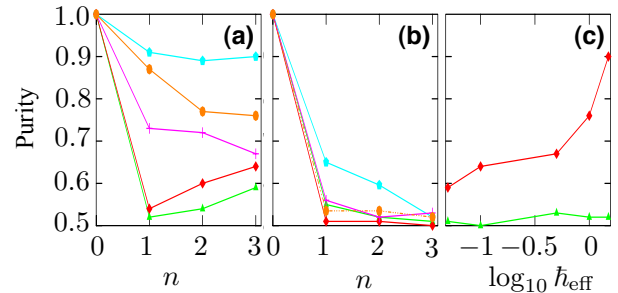


FIG. 4: **Purity loss of the diagonal polarization state for regular and chaotic dynamics of the environment.** **a,b**, Purity as a function of the number of KHO iterations,  $n$ , for regular dynamics ( $K = 0.5$ ), and chaotic dynamics ( $K = 2$ ), respectively. In both figures  $\alpha = 2\pi/3$ , and  $\hbar_{\text{eff}} = 0.05$  (green triangles),  $0.1$  (red squares),  $0.5$  (purple crosses),  $1.0$  (orange circles), and  $1.5$  (blue polygons). **c**, The final purity as a function of  $\hbar_{\text{eff}}$  for  $n = 3$  KHO iterations, with  $K = 2$  (green triangles) and  $K = 0.5$  (red squares).

chaotic dynamics ( $K = 2$ ). In the latter, for all values of  $\hbar_{\text{eff}}$ , rapid loss of purity occurs while the state becomes nearly maximally entangled (purity equal to  $1/2$ ). Fig. 4(c) shows the final purity for  $n = 3$  kicks as a function of  $\hbar_{\text{eff}}$  for  $K = 2$  (green triangles) and  $K = 0.5$  (red squares). The results show that the entanglement between the qubit and the environment depends strongly on the effective Planck constant for regular dynamics ( $K = 0.5$ ), and this dependence is much weaker for the chaotic case ( $K = 2$ ).

Our approach allows for the study of the dynamics of a non-relativistic quantum system using an intense classical laser

beam due to the analogy between quantum mechanics and classical wave mechanics. A possible next step is to study the chaotic evolution of entangled photons. The optical realization of non-linear quantum dynamics should prove invaluable in the experimental investigation of quantum chaos, decoherence, and the quantum-classical boundary.

## Supplementary Material

### Method to Measure the Optical Wigner Function

The method used to directly measure the optical Wigner function is an interferometric scheme proposed in reference [30]. The interferometer is illustrated in Figure 1 of the manuscript. The displacement and tilting of a steering mirror ( $M1$ ) at the entrance of a three-mirror Sagnac interferometer displaces the optical field by  $Q$  and changes its direction of propagation by  $P$  (which in the paraxial approximation corresponds to the addition of a phase). This produces the field  $\exp(i\hbar_{\text{eff}}P\xi/2)\Psi(Q + \xi/2, z)$ .

A polarizing beam-splitter divides the field into two spatially identical components and a Dove prism ( $DP2$ ) placed inside the interferometer realizes opposite  $90^\circ$  spatial rotations in the two counter-propagating transverse spatial modes, resulting in a total relative rotation by  $180^\circ$ . The modes are recombined, and projected onto the diagonal polarization direction before detection by an area-integrating ‘‘bucket’’ detector. The measured intensity is composed of three terms  $I = I_1 + I_2 + I_{\text{int}}$ , where the sum  $I_1 + I_2$  is constant and equals half the total input intensity. The term  $I_{\text{int}}$  originates from the interference between the counter-propagating beams. Due to the relative rotation implemented by  $DP2$ ,  $I_{\text{int}}$  is proportional to:

$$\mathcal{W}(Q, P) = A \int_{-\infty}^{\infty} \Psi\left(Q + \frac{\xi}{2}\right) \Psi^*\left(Q - \frac{\xi}{2}\right) e^{i\hbar_{\text{eff}}P\xi} d\xi, \quad (7)$$

The right-hand side of Eq.(7) is an integral over spatial variable  $\xi$  of the overlap between the displaced field,  $\exp(i\hbar_{\text{eff}}P\xi/2)\Psi(Q + \xi/2, z)$ , and its complex conjugate with the transformation  $\xi \rightarrow -\xi$ . This transformation corresponds to the  $180^\circ$  relative rotation implemented by  $DP2$ . It is important to note that astigmatic effects introduced by the Dove prism [42] inside the Sagnac interferometer does not alter the measured Wigner function [43].

In this way, the amplitude of the optical Wigner function at point  $(Q, P)$  can be obtained by measuring the intensity at the interferometer output, for different settings of the tilt angle and displacement of the steering mirror  $M1$ . In our experiment these parameters were controlled with high resolution motorized stages. At the exit of the interferometer we use a quarter wave plate (QWP) that is tilted to correct the polarization aberrations introduced by  $DP2$  inside the interferometer [44]. Detailed calculations of the light propagation in the interferometer, and how the optical spatial Wigner function

arises from the area integrated intensity measurements can be found in [43].

### Analysis of the Experimental Data

The final state of the optical KHO is obtained at the output plane  $z_0$ , indicated in Figure 1(b) of the manuscript. However, the optical wave-function propagates through free space and several linear optical elements before reaching the steering mirror at the entrance of the Sagnac interferometer, where the optical Wigner function is measured. One must therefore take into account this evolution before comparing measurements with the theoretical Wigner functions, obtained from numerical calculation of the quantum KHO evolution. This is done by calculating the total linear transformation  $\mathbb{M}$ , resulting from propagation through all of the optical elements and free space between the output plane  $z_0$  and the steering mirror shown in Figure 1 (b).

The expected Wigner function in the measurement plane can be written as

$$W(x, p_x) = W_x^{(\text{KHO})}(x', p'_x) \times W_y^{(\text{Gauss})}(y', p'_y), \quad (8)$$

where  $(x' \ y' \ p'_x \ p'_y)^T = \mathbb{M}^{-1}(x \ 0 \ p_x \ 0)^T$  are the transformed coordinates. The function  $W_x^{(\text{KHO})}(x, p_x)$  represents the Wigner function due to KHO evolution of the initial Gaussian state implemented in the  $x$  transverse spatial direction. The function  $W_y^{(\text{Gauss})}(y, p_y)$  refers to the Gaussian state describing the  $y$  transverse spatial direction at plane  $z_0$ . This spatial mode does not undergo KHO the evolution.

Experimental errors associated to the propagation through the optical elements between the output plane  $z_0$  and the steering mirror results in scaling, skewing and rotation of the final measured Wigner Function,  $W^{(\text{exp})}(x, p_x)$ , in comparison to  $W^{(\text{KHO})}(x, p_x)$ . These uncertainties are due principally to errors in lens placement, misalignment of the optical elements, and diffraction. Nevertheless, a single linear transformation  $\mathbb{E}$  corrects these errors, such that  $W^{(\text{exp})}(x, p_x) = W^{(\text{KHO})}(\mathbb{E}(x, p_x))$ . Both  $\mathbb{M}$  and  $\mathbb{E}$  depend only on the experimental setup, and are the same for all measurements of Wigner functions, including the case in which the spatial light modulator is turned off. In this case, the implemented evolution is that of a simple harmonic oscillator (SHO). With the KHO turned off, we determined the value of  $\mathbb{E}$ , and used these values to correct all of the KHO Wigner functions. This was repeated for each harmonic evolution used.

### Using the spatial light modulator to implement a dephasing-type decoherence channel

The spatial light modulator (SLM) imprints a phase on the horizontal polarization component of the light beam, but leaves the phase of the vertical polarization component unchanged. Without the SLM, the optical system is designed to

implement SHO evolution via the fractional Fourier transform systems composed of the cylindrical lens and free-space propagation. Therefore, if diagonally polarized light is used in the KHO optical setup, one obtains the transformation:

$$|\Psi\rangle \otimes |+\rangle \rightarrow \frac{1}{\sqrt{2}} (U_{\text{KHO}}|\Psi\rangle \otimes |H\rangle + U_{\text{SHO}}|\Psi\rangle \otimes |V\rangle) \quad (9)$$

where  $|+\rangle = (|H\rangle + |V\rangle)/\sqrt{2}$ , and  $|\Psi\rangle$  designates the transverse spatial mode of the light beam. The evolution operators  $U_{\text{KHO}}$  and  $U_{\text{SHO}}$  act on the spatial degree of freedom, and correspond to the evolution of the KHO and the SHO, respectively. The total evolution given in Eq.(9) could be interpreted as the quantum evolution of a qubit interacting with a quantum KHO via a dephasing-type of coupling of the form  $(K \cos Q)/2|H\rangle\langle H|$ .

Performing a polarization measurement of the output beam using a “bucket” detector is equivalent to tracing over the spatial degree of freedom, and yields,

$$\rho = \frac{1}{2} (|H\rangle\langle H| + |V\rangle\langle V| + f|H\rangle\langle V| + f^*|V\rangle\langle H|), \quad (10)$$

where  $f = \langle \Psi | U_{\text{SHO}}^\dagger U_{\text{KHO}} | \Psi \rangle$  is the overlap between the SHO and KHO quantum states. The purity of the polarization state is given by  $\text{Tr}\rho^2 = (1 + |f|^2)/2$ , and decays with  $f$  [38].

We use wave plates and a polarizing beam splitter, to perform quantum polarization state tomography using the standard recipe [45, 46] to obtain the density matrix  $\rho$ , from which we calculate the results shown in Figure 4.

---

\* gabibl@if.ufrj.br

- [1] H-J. Stöckmann. *Quantum Chaos, An introduction*. Cambridge University Press, Cambridge, 1999.
- [2] Wojciech Hubert Zurek and Juan Pablo Paz. Decoherence, chaos, and the second law. *Phys. Rev. Lett.*, 72:2508–2511, 1994.
- [3] F. L. Moore, J. C. Robinson, C. F. Bharucha, Bala Sundaram, and M. G. Raizen. Atom optics realization of the quantum  $\delta$ -kicked rotor. *Phys. Rev. Lett.*, 75(25):4598–4601, 1995.
- [4] D.A. Steck, W.H. Oskay, and M.G. Raizen. Observation of chaos-assisted tunneling between islands of stability. *Science*, 293(5528):274, 2001.
- [5] WK Hensinger, H Häffner, and A Browaeys. Dynamical tunnelling of ultracold atoms. *Nature*, 2001.
- [6] S. Chaudhury, A. Smith, B. E. Anderson, S. Ghose, and P. S. Jessen. Quantum signatures of chaos in a kicked top. *Nature*, 461(7265):768–771, 2009.
- [7] Julien Chabé, Gabriel Lemarié, Benoît Grémaud, Dominique Delande, Pascal Szriftgiser, and Jean Garreau. Experimental Observation of the Anderson Metal-Insulator Transition with Atomic Matter Waves. *Physical Review Letters*, 101(25):255702, December 2008.
- [8] Mark Sadgrove and Sandro Wimberger. Chapter 7 - a pseudoclassical method for the atom-optics kicked rotor: from theory to experiment and back. In P.R. Berman E. Arimondo and C.C. Lin, editors, *Advances in Atomic, Molecular, and Optical Physics*, volume 60 of *Advances In Atomic, Molecular, and Optical Physics*, pages 315 – 369. Academic Press, 2011.
- [9] S Schlunk, M d’Arcy, S Gardiner, and G Summy. Experimental observation of high-order quantum accelerator modes. *Physical Review Letters*, 90(12), March 2003.
- [10] C. Ryu, M. F. Andersen, A. Vaziri, M. B. d’Arcy, J. M. Grossman, K. Helmerson, and W. D. Phillips. High-order quantum resonances observed in a periodically kicked bose-einstein condensate. *Phys. Rev. Lett.*, 96(16):160403, 2006.
- [11] Tal Schwartz, Guy Bartal, Shmuel Fishman, and Mordechai Segev. Transport and Anderson localization in disordered two-dimensional photonic lattices. *Nature*, 446(7131):52–55, mar 2007.
- [12] B Fischer, A. Rosen, A. Bekker, and S Fishman. Experimental observation of localization in the spatial frequency domain of a kicked optical system. *Physical Review E*, 61(5):4694–4697, 2000.
- [13] Felix M. Izrailev. Simple models of quantum chaos: Spectrum and eigenfunctions. *Physics Reports*, 196(5-6):299 – 392, 1990.
- [14] Giulio Casati and Boris Chirikov, editors. *Quantum Chaos: Between Order and Disorder*. Cambridge University Press, Cambridge, 1995.
- [15] RE Prange. Experimental realizations of kicked quantum chaotic systems. *Physical Review Letters*, 1989.
- [16] M.V. Berry, N.L. Balazs, M. Tabor, and A. Voros. Quantum maps. *Annals of Physics*, 122(1):26 – 63, 1979.
- [17] J. H. Hannay, J. P. Keating, and Alfredo M. Ozorio de Almeida. Optical realization of the baker’s transformation. *Nonlinearity*, 7(8):1327–1342, 1994.
- [18] G.M. Zaslavsky, R.Z. Sagdeev, D.A. Usikov, and A.A. Chernikov. *Weak Chaos and Quasi-Regular Patterns*. Cambridge University Press, Cambridge, 1991.
- [19] T. M. Fromhold, A. A. Krokhin, C. R. Tench, S. Bujkiewicz, P. B. Wilkinson, F. W. Sheard, and L. Eaves. Effects of stochastic webs on chaotic electron transport in semiconductor superlattices. *Physical Review Letters*, 87(4):046803, 2001.
- [20] T. M. Fromhold, A. Patane, S. Bujkiewicz, P. B. Wilkinson, D. Fowler, D. Sherwood, S. P. Stapleton, A. A. Krokhin, L. Eaves, M. Henini, N. S. Sankeshwar, and F. W. Sheard. Chaotic electron diffusion through stochastic webs enhances current flow in superlattices. *Nature*, 428:726–730, 2004.
- [21] S. A. Gardiner, J. I. Cirac, and P. Zoller. Quantum chaos in an ion trap: The delta-kicked harmonic oscillator. *Physical Review Letters*, 79(24):4790–4793, 1997.
- [22] R. Artuso, F. Borgonovi, I. Guarneri, L. Rebuzzini, and G Casati. Phase Diagram in the kicked Harper model. *Physical Review Letters*, 69(23):3302–3305, 1992.
- [23] A Carvalho and A Buchleitner. Web-assisted tunneling in the kicked harmonic oscillator. *Physical Review Letters*, 2004.
- [24] R. Artuso and L Rebuzzini. Nonlinearity effects in the kicked oscillator. *Physical Review E*, 66(1):017203, 2002.
- [25] F. Borgonovi and L. Rebuzzini. Translational invariance in the kicked harmonic oscillator. *Physical Review E*, 52:2302–2309, 1995.
- [26] David Stoler. Operator methods in physical optics. *Journal of the Optical Society of America*, 71(3):334–341, 1981.
- [27] M. Nazarathy and J. Shamir. First-order optics - a canonical operator representation: Lossless systems. *Journal of the Optical Society of America A*, 72(3):356–364, 1982.
- [28] H.M. Ozaktas, Z. Zalevsky, and M. Apler Kutay. *The Fractional Fourier Transform: with Applications in Optics and Signal Processing*. John Wiley and Sons Ltd., West Sussex, 2001.
- [29] M.J. Bastiaans. The wigner distribution function applied to optical signals and systems. *Optics Communications*, 25(1):26 –

- 30, 1978.
- [30] Eran Mukamel, Konrad Benaszek, Ian A. Walmsley, and Christophe Dorrer. Direct measurement of the spatial wigner function with area-integrated detection. *Optics Letters*, 28(15):1317–1319, 2003.
- [31] W.H. Zurek. Sub-planck structure in phase space and its relevance to quantum decoherence. *Nature*, 412:712–717, 2001.
- [32] W.H. Zurek. Decoherence, einselection, and the quantum origins of the classical. *Rev. Mod. Phys.*, 75(3):715–775, 2003.
- [33] F Toscano, R de Matos Filho, and L Davidovich. Decoherence and the quantum-classical limit in the presence of chaos. *Physical Review A*, 71(1), 2005.
- [34] Raphael N P Maia, Fernando Nicacio, Raúl O Vallejos, and Fabricio Toscano. Semiclassical propagation of gaussian wave packets. *Physical Review Letters*, 100(18):184102, 2008.
- [35] Roman Schubert, Raúl O Vallejos, and Fabricio Toscano. How do wave packets spread? Time evolution on Ehrenfest time scales. *Journal Of Physics A-Mathematical And Theoretical*, 45(21):215307, May 2012.
- [36] T Gorin, C Pineda, H Kohler, and TH Seligman. A random matrix theory of decoherence. *New Journal of Physics*, 10:115016, 2008.
- [37] Giuliano Benenti. Entanglement, randomness and chaos. *Riv. Nuovo Cimento*, 35:105, 2009. arXiv:0807.4364v2.
- [38] G.B. Lemos and Fabricio Toscano. Decoherence, entanglement decay, and equilibration produced by chaotic environments. *Physical Review E*, 84:016220, 2011.
- [39] Jae Weon Lee, Dmitri V. Averin, Giuliano Benenti, and Dima L. Shepelyansky. Model of a deterministic detector and dynamical decoherence. *Physical Review A*, 72(1):012310, 2005.
- [40] Leonardo Ermann, Juan Pablo Paz, and Marcos Saraceno. Decoherence induced by a chaotic environment: A quantum walker with a complex coin. *Physical Review A*, 73(1):012302, 2006.
- [41] K.M. Fonseca Romero *et al.* An analytical relation between entropy production and quantum lyapunov exponents for gaussian bipartite systems. *J. Phys. A: Math. Theor.*, 41:115303, 2008.
- [42] N González, G Molina-Terriza, and JP Torres. How a Dove prism transforms the orbital angular momentum of a light beam. *Opt. Express*, 14:9093–9102, 2006.
- [43] G. B. Lemos and Fabricio Toscano. On an interferometric technique to measure the space-spatial frequency optical wigner function. In preparation.
- [44] I. Moreno, G. Paez, and M. Strojnik. Polarization transforming properties of dove prisms. *Optics Communications*, 220:257–268, 2003.
- [45] Michael A. Nielsen and Isaac Chuang. *Quantum Computation and Quantum Information*. Cambridge University Press, Cambridge, 2000.
- [46] Daniel F. V. James, Paul G. Kwiat, William J. Munro, and Andrew G. White. Measurement of qubits. *Phys. Rev. A*, 64:052312, 2001.